PERGAMON

International Journal of Heat and Mass Transfer 46 (2003) 999–1011

International Journal of HEAT and MASS TRANSFER

www.elsevier.com/locate/ijhmt

Effects of mass transfer on the transient free convection flow of a dissipative fluid along a semi-infinite vertical plate with constant heat flux

M.Y. Gokhale [a,*], Fathia Moh. Al Samman [b]

[a] Department of Mathematics, Maharashtra Institute of Technology, Kothrud, Pune 411 038, India
[b] Department of Mathematics, University of Pune, Pune 411 007, India

Received 27 February 2002; received in revised form 2 September 2002

Abstract

Effect of mass transfer on the transient free convection flow of a dissipative fluid along a semi-infinite vertical plate in presence of constant heat flux, is studied by solving coupled non-linear system of partial differential equations, using Crank–Nicolson technique which is stable and convergent. Transient temperature, concentration and velocity profiles, local and average skin-friction, Nusselt number and Sherwood number are shown graphically for air. The effects of ε, viscous dissipative parameter, Schmidt number, buoyancy ratio parameter on the transient state are discussed.

1. Introduction

Many papers have been published on steady free convection flow of a viscous incompressible fluid along a semi-infinite vertical plate because of its wide industrial applications. These are discussed in a book published by Gebhart et al. [1]. In the absence of viscous dissipation, the earliest solution to this problem was presented by Pohlhausen [2] using momentum integral method whereas the numerical solution to similarity equations was first presented by Ostrach [3], assuming isothermal plate. But Gebhart [4], first showed the importance of viscous dissipation in free convection flow along a semi-infinite vertical isothermal plate and presented a similarity solution by defining a dissipation parameter $\varepsilon = g\beta L/c_p$, which is the ratio of the kinetic energy of the flow to the heat transferred to the fluid.

Another problem of interest is, unsteady free convection (also known as transient free convection) flow along a vertical semi-infinite isothermal plate. In this case, it is important to know the time required for the unsteady flow to reach steady state. The first attempt in this direction was made by Callahan and Marner [5] who solved the non-linear system of equations by explicit finite difference scheme. The solution by this technique is not always convergent and one has to establish the convergence for stability of this explicit finite difference scheme. Callahan and Marner [5] also considered the presence of mass transfer and showed that the explicit finite difference scheme was convergent and stable for Prandtl number unity and Schmidt number $Sc = 0.2$, 0.7, 7.0. However, the Schmidt number Sc of foreign masses for air ($Pr = 0.71$) and water ($Pr = 7.0$) is quite different for different substances and hence Callahan and Marner's [5] analysis is rather restricted. Also their explicit finite difference scheme was not shown to be convergent and stable for $Pr \neq 1.0$ Soundalgekar and Ganesan [6] restudied the same problem by implicit finite difference scheme which is always stable and convergent for all values of the Prandtl number and compared their results with those of Callahan and Marner [5] and the agreement was excellent.

Later on, Soundalgekar and Ganesan [7–9] studied the problem of transient free convection flow along a semi-infinite vertical plate under different conditions. In

* Corresponding author. Fax: +91-020-544-2770.
E-mail addresses: mukundyg@yahoo.com (M.Y. Gokhale), mfathia@yahoo.com (F.M. Al Samman).

0017-9310/03/$ - see front matter
PII: S0017-9310(02)00367-8

Nomenclature

c	species concentration in fluid
c_∞	species concentration in fluid far away from the plate
c_w	species concentration at the plate
C	non-dimensional species concentration
c_p	specific heat at constant pressure
D	chemical molecular diffusivity
Gr_L	Grashof number
Gr_c	modified Grashof number
g	acceleration due to gravity
K	thermal conductivity
L	length of the plate
Nu_{XL}	local Nusselt number
$\overline{Nu}_X$	average Nusselt number
N	buoyancy ratio parameter
Pr	Prandtl number
Sh_{XL}	local Sherwood number
$\overline{Sh}_X$	average Sherwood number
Sc	Schmidt number
T	temperature of the fluid
T_∞	temperature of the fluid far away from the plate
T_w	plate temperature
t'	time
t	non-dimensional time
u, v	velocity components in the x and y-directions
U, V	non-dimensional velocity components
X, Y	coordinates axes
β	coefficient of volume expansion
β^*	volumetric coefficient of expansion with concentration
μ	dynamic viscosity
ν	kinematic viscosity
ρ	density
α	thermal diffusivity $K/\rho c_p$
τ_L	local skin-friction
$\bar{\tau}$	average skin-friction
ε	dissipation parameter
θ	non-dimensional temperature

their paper [7], transient free convection flow along an isothermal semi-infinite vertical plate was studied, and in the paper [8], the effects of mass transfer on the transient free convection flow along an isothermal plate were studied whereas in the paper [9], the transient free convection flow along a semi-infinite vertical plate in the presence of constant heat flux was studied. Again in all these papers, the stability and convergence of the implicit finite difference scheme was separately established. In another paper by Soundalgekar et al. [10], the effects of viscous dissipative heat on the transient free convection flow along a semi-infinite isothermal plate were studied. Because of technological importance it is now proposed to study the effects of mass transfer on the transient free convection flow of a dissipative fluid along a semi-infinite vertical plate in the presence of a constant heat flux. The non-linear system of partial differential equations are solved by implicit finite difference scheme of Crank–Nicolson type and the effects of mass transfer and viscous dissipative heat on time to reach the steady state are studied. In Section 2, the mathematical analysis is presented and in Section 3, the conclusions are setout.

2. Mathematical analysis

We consider the flow of a viscous incompressible fluid containing foreign mass like CO_2, H_2O (water vapor) etc. past a semi-infinite vertical plate such that the plate, fluid and the foreign mass are at the same temperature T_∞ and the concentration level C_∞. At time $t' > 0$, the plate is supplied heat at constant rate and the concentration level near the plate is raised from C_∞ to C_w. The x-axis is taken along the plate in the vertically upward direction and the y-axis is taken normal to the plate. Then under the usual Boussinesq's approximation, with low concentration level, the flow can be shown to be governed by following boundary layer equations:

$$\frac{\partial u}{\partial x}+\frac{\partial v}{\partial y}=0 \tag{1}$$

$$\frac{\partial u}{\partial t'}+u\frac{\partial u}{\partial x}+v\frac{\partial \mathrm{u}}{\partial \mathrm{y}}=\nu\frac{\partial^2 u}{\partial y^2}+g\beta(T-T_\infty)+g\beta^*(c-c_\infty) \tag{2}$$

$$\frac{\partial T}{\partial t'}+u\frac{\partial T}{\partial x}+v\frac{\partial T}{\partial y}=\alpha\frac{\partial^2 T}{\partial y^2}+\frac{\mu}{\rho c_p}\left(\frac{\partial u}{\partial y}\right)^2 \tag{3}$$

$$\frac{\partial c}{\partial t'}+u\frac{\partial c}{\partial x}+v\frac{\partial c}{\partial y}=D\frac{\partial^2 c}{\partial y^2} \tag{4}$$

with the following initial and boundary conditions:

$$\begin{aligned}
&t'\leqslant 0, \quad u=0, \quad v=0, \quad T=T_\infty, \quad c=c_\infty, \quad \text{for all } y\\
&t'>0, \quad u=0, \quad v=0, \quad T=T_\infty, \quad c=c_\infty, \quad \text{at } x=0\\
&u=0, \quad v=0, \quad \frac{\partial T}{\partial y}=\frac{-q}{k}, \quad c=c_w, \quad \text{at } y=0\\
&u=0, \quad T\to T_\infty, \quad c\to c_\infty \quad \text{as } y\to\infty
\end{aligned} \tag{5}$$

All the physical variables are defined in the Nomenclature.

We now introduce the following non-dimensional quantities:

$$\begin{aligned} &U=\frac{uL}{vGr^{1/2}}, \quad V=\frac{vL}{vGr^{1/4}}, \quad X=\frac{x}{L} \\ &Y=\frac{y}{LGr^{-1/4}}, \quad \theta=\frac{T-T_\infty}{qL/kGr^{1/4}}, \quad C=\frac{c-c_\infty}{c_w-c_\infty} \\ &Gr=\frac{g\beta L^4 q}{kv^2}, \quad Pr=\frac{v}{\alpha}, \quad Sc=\frac{v}{D}, \quad \varepsilon=\frac{g\beta L}{c_p} \\ &N=\frac{\beta^*(c_w-c_\infty)k}{\beta q L}, \quad t=\frac{t' vGr^{1/2}}{L^2} \end{aligned} \tag{6}$$

in Eqs. (1)–(5) which then reduce to following:

$$\frac{\partial U}{\partial X}+\frac{\partial V}{\partial Y}=0 \tag{7}$$

$$\frac{\partial U}{\partial t}+U\frac{\partial U}{\partial X}+V\frac{\partial U}{\partial Y}=\frac{\partial^2 U}{\partial Y^2}+Gr^{-1/4}\theta+NC \tag{8}$$

$$\frac{\partial \theta}{\partial t}+U\frac{\partial \theta}{\partial X}+V\frac{\partial \theta}{\partial Y}=\frac{1}{Pr}\frac{\partial^2 \theta}{\partial Y^2}+\varepsilon Gr^{1/4}\left(\frac{\partial U}{\partial Y}\right)^2 \tag{9}$$

$$\frac{\partial C}{\partial t}+U\frac{\partial C}{\partial X}+V\frac{\partial C}{\partial Y}=\frac{1}{Sc}\frac{\partial^2 C}{\partial Y^2} \tag{10}$$

where $\varepsilon = g\beta L/c_p$ is a dissipation parameter as introduced by Gebhart [4]. The initial and boundary conditions are now

$$\begin{aligned} &t\leqslant 0, \quad U=V=\theta=C=0 \\ &t>0, \quad U=V=\theta=C=0 \quad \text{at } X=0 \\ &U=V=0, \quad \frac{\partial\theta}{\partial Y}=-1, \quad C=1 \quad \text{at } Y=0 \\ &U=\theta=C=0 \quad \text{as } Y\to\infty \end{aligned} \tag{11}$$

We now have to solve the coupled non-linear partial differential equations by an implicit finite difference method of the Crank–Nicolson type. Taking length of the semi-infinite plate as $L=1$, we consider a rectangular region with X varying from 0 to 1 and Y varying from 0 to $Y_{\max}=16$, where $X=1$ corresponds to the height of the plate and $Y_{\max}$ is regarded as ∞. It is ensured that $Y_{\max}$ lies well outside the momentum and thermal boundary layers. We now divide X and Y-directions into M and N grid-spacing respectively. We select mesh size in the X and Y-directions as follows:

$$\begin{aligned} &\Delta X=0.05 \\ &\Delta Y=0.25 \\ &\Delta t=0.01 \end{aligned} \tag{12}$$

The implicit finite difference equation of Crank–Nicolson type corresponding to Eq. (9) is

$$\begin{aligned} &\frac{\theta_{i,j}^{n+1}-\theta_{i,j}^{n}}{\Delta t}+\frac{U_{i,j}^{n}}{2}\left[\frac{\theta_{i,j}^{n+1}-\theta_{i-1,j}^{n+1}+\theta_{i,j}^{n}-\theta_{i-1,j}^{n}}{\Delta X}\right] \\ &\quad+\frac{V_{i,j}^{n}}{4}\left[\frac{\theta_{i,j+1}^{n+1}-\theta_{i,j-1}^{n+1}+\theta_{i,j+1}^{n}-\theta_{i,j-1}^{n}}{\Delta Y}\right] \\ &\quad=\frac{1}{2Pr}\left[\frac{\theta_{i,j-1}^{n+1}-2\theta_{i,j}^{n+1}+\theta_{i,j+1}^{n+1}+\theta_{i,j-1}^{n}-2\theta_{i,j}^{n}+\theta_{i,j+1}^{n}}{(\Delta Y)^2}\right] \\ &\quad+\varepsilon Gr^{1/4}\left[\frac{U_{i,j+1}^{n}-U_{i,j}^{n}}{\Delta Y}\right]^2 \end{aligned} \tag{13}$$

The boundary condition $\partial\theta/\partial Y=-1$ takes the following form

$$\frac{\theta_{i,1}^{n+1}-\theta_{i,-1}^{n+1}+\theta_{i,+1}^{n}-\theta_{i,-1}^{n}}{4\Delta Y}=-1 \tag{14}$$

From Eqs. (13) and (14), we have

$$\begin{aligned} \frac{\theta_{i,0}^{n+1}-\theta_{i,0}^{n}}{\Delta t}&=\frac{1}{Pr}\left[\frac{2\Delta Y+\theta_{i,1}^{n+1}+\theta_{i,1}^{n}-\theta_{i,0}^{n+1}-\theta_{i,0}^{n}}{(\Delta Y)^2}\right] \\ &\quad+\varepsilon Gr^{1/4}\left[\frac{U_{i,1}^{n}-U_{i,0}^{n}}{\Delta Y}\right]^2 \end{aligned} \tag{15}$$

Eq. (15) now reduces to

$$A_1\theta_{i,j-1}^{n+1}+B_1\theta_{i,j}^{n+1}+D_1\theta_{i,j+1}^{n+1}=E_1 \tag{16}$$

where

$$A_1=-\frac{V_{i,j}^{n}}{4\Delta Y}-\frac{1}{2Pr(\Delta Y)^2}$$

$$B_1=\frac{1}{\Delta t}+\frac{U_{i,j}^{n}}{2\Delta X}+\frac{1}{Pr(\Delta Y)^2}$$

$$D_1=\frac{V_{i,j}^{n}}{4\Delta Y}-\frac{1}{2Pr(\Delta Y)^2}$$

$$\begin{aligned} E_1&=\frac{1}{\Delta t}\theta_{i,j}^{n}+\frac{U_{i,j}^{n}}{2}\left[\frac{\theta_{i-1,j}^{n+1}-\theta_{i,j}^{n}+\theta_{i-1,j}^{n}}{\Delta X}\right] \\ &\quad-\frac{V_{i,j}}{4}\left(\frac{\theta_{i,j+1}^{n}-\theta_{i,j-1}^{n}}{\Delta Y}\right)+\frac{1}{2Pr}\left[\frac{\theta_{i,j-1}^{n}-2\theta_{i,j}^{n}+\theta_{i,j+1}^{n}}{(\Delta Y)^2}\right] \\ &\quad+\varepsilon Gr^{1/4}\left[\frac{U_{i,j+1}^{n}-U_{i,j}^{n}}{\Delta Y}\right]^2 \end{aligned}$$

Similarly, the finite difference equation corresponding to differential equation (10) reduces to

$$A_2C_{i,j-1}^{n+1}+B_2C_{i,j}^{n+1}+D_2C_{i,j+1}^{n+1}=E_2 \tag{17}$$

where

$$A_2=-\frac{V_{i,j}^{n}}{4\Delta Y}-\frac{1}{2Sc(\Delta Y)^2}$$

$$B_2 = \frac{1}{\Delta t} + \frac{U^n_{i,j}}{2\Delta X} + \frac{1}{Sc(\Delta Y)^2}$$

$$D_2 = \frac{V^n_{i,j}}{4\Delta Y} - \frac{1}{2Sc(\Delta Y)^2}$$

$$E_2 = \frac{1}{\Delta t}C^n_{i,j} + \frac{U^n_{i,j}}{2}\left[\frac{C^{n+1}_{i-1,j} - C^n_{i,j} + C^n_{i-1,j}}{\Delta X}\right] - \frac{V_{i,j}}{4}\left(\frac{C^n_{i,j+1} - C^n_{i,j-1}}{\Delta Y}\right) + \frac{1}{2Sc}\left[\frac{C^n_{i,j-1} - 2C^n_{i,j} + C^n_{i,j+1}}{(\Delta Y)^2}\right]$$

Again, the finite difference equation corresponding to Eq. (8) is

$$A_3 U^{n+1}_{i,j-1} + B_3 U^{n+1}_{i,j} + D_3 U^{n+1}_{i,j+1} = E_3 \tag{18}$$

where

$$A_3 = -\frac{V^n_{i,j}}{4\Delta Y} - \frac{1}{2(\Delta Y)^2}$$

$$B_3 = \frac{1}{\Delta t} + \frac{U^n_{i,j}}{2\Delta X} + \frac{1}{(\Delta Y)^2}$$

$$D_3 = \frac{V^n_{i,j}}{4\Delta Y} - \frac{1}{2(\Delta Y)^2}$$

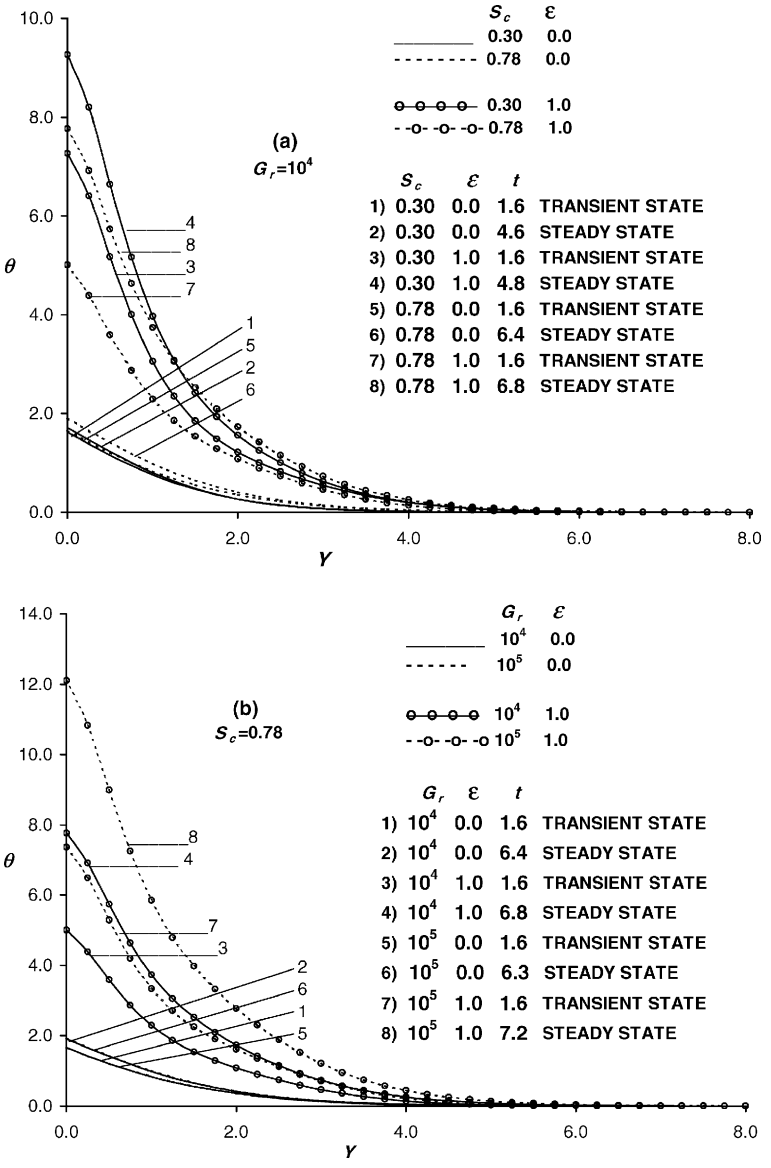

Fig. 1. Transient temperature profiles $X = 1.0$, $Pr = 0.733$, $N = 2.0$.

$$E_3 = \frac{1}{\Delta t}U_{i,j}^n + \frac{U_{i,j}^n}{2}\left[\frac{U_{i-1,j}^{n+1} - U_{i,j}^n + U_{i-1,j}^n}{\Delta X}\right] - \frac{V_{i,j}}{4}\left(\frac{U_{i,j+1}^n - U_{i,j-1}^n}{\Delta Y}\right) + \frac{1}{2}\left[\frac{U_{i,j-1}^n - 2U_{i,j}^n + U_{i,j+1}^n}{(\Delta Y)^2}\right]Gr^{-1/4}\frac{\theta_{i,j}^{n+1} + \theta_{i,j}^n}{2} + N\frac{C_{i,j}^{n+1} + C_{i,j}^n}{2}$$

Then the finite difference equation corresponding to Eq. (7) is

$$V_{i,j}^{n+1} = E_4 \tag{19}$$

where

$$E_4 = V_{i,j-1}^{n+1} - V_{i,j+1}^n + V_{i,j-1}^n - \frac{\Delta Y}{2\Delta X}\left[U_{i,j}^{n+1} - U_{i-1,j}^{n+1} + U_{i,j}^n - U_{i-1,j}^n + U_{i,j-1}^{n+1} - U_{i-1,j-1}^{n+1} + U_{i,j-1}^n - U_{i-1,j-1}^n\right]$$

The initial and boundary conditions now take the following form

$$\begin{aligned} &U_{i,j}^0 = 0, \quad U_{i,0}^n = 0, \quad U_{0,j}^n = 0, \quad U_{i,N}^n = 0 \\ &V_{i,j}^0 = 0, \quad V_{i,0}^n = 0, \quad V_{0,j}^n = 0 \\ &C_{i,j}^0 = 0, \quad C_{i,0}^n = 1, \quad C_{0,j}^n = 0, \quad C_{i,N}^n = 0 \\ &\theta_{i,j}^0 = 0, \quad \frac{\theta_{i,1}^{n+1} - \theta_{i,-1}^{n+1} + \theta_{i,+1}^n - \theta_{i,-1}^n}{4\Delta Y} = -1 \\ &\theta_{0,j}^n = 0, \quad \theta_{i,N}^n = 0 \end{aligned} \tag{20}$$

Here the subscript i designates the grid-point with X-coordinate $\sum_{k=1}^{i}\Delta X_k$, j designates the grid-point with Y-coordinate $\sum_{k=1}^{j}\Delta Y_k$, and the subscript n designates a value of time $t = n\Delta t$.

Now during the computations, the coefficients $U_{i,j}^n$, $V_{i,j}^n$ appearing in Eqs. (16) and (17) are treated as constants during a given time-step. The values of U, V, θ and C are known at all grid-points at $\tau = 0$ from the initial conditions. We then calculate the values of U, V, θ and C at $\tau = \Delta t$ as follows:

On the line $i = 1$, Eq. (16) constitutes a tridiagonal system of equations for $j = 1$ to $N - 1$ in $N - 1$ unknowns, which are solved by using the Thomas algorithm described in Carnahan et al. [11].

We have thus computed the values of θ, C and then U on the line $i = 1$. This helps us to compute the values of V from Eq. (19). This procedure is repeated for finding the values of θ, C, U and V on all i-lines.

In this way, the procedure is repeated for $n = 2, 3, 4, \ldots$ until the steady state is reached. The steady state is determined when the difference between two consecutive values of U or θ or C or V is less than 10^{-6}.

We have computed the time required to reach the steady state for different values of N, Gr, Sc and ε when $Pr = 0.733$ (air). Here N is the buoyancy ratio force and is known as aiding force when $N > 0$ and opposing one when $N < 0$. We are considering here only values of $N > 0$. Also, the Schmidt number Sc for air is defined by Gebhart and Pera [12], and we have taken only $Sc = 0.30$ and 0.78. The numerical values of U, θ and C are computed at $X = 1.0$ only. Initially time step Δt was chosen as 0.02 and time required to reach steady state was calculated. Then to check the accuracy of the result,

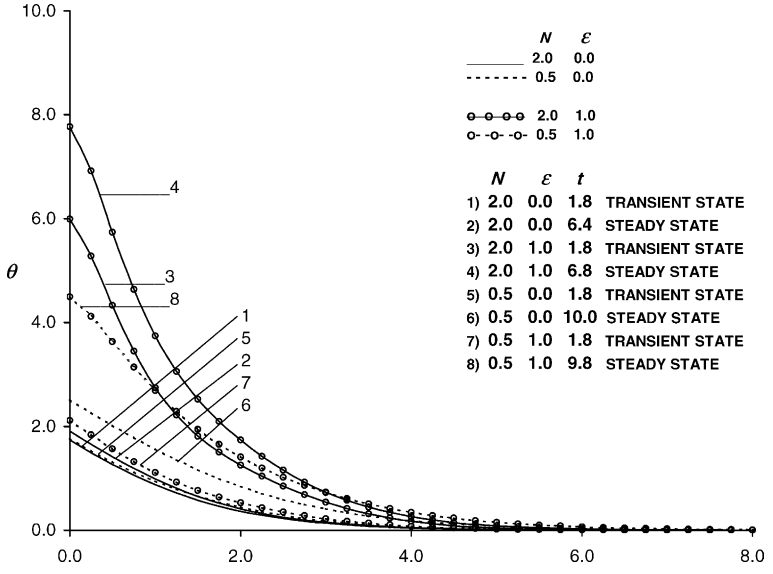

Fig. 2. Transient temperature profiles $X = 1.0$, $Pr = 0.733$, $Sc = 0.78$, $Gr = 10^4$.

Δt was chosen as 0.01 and 0.04. The time required to reach steady state remained unchanged.

In Fig. 1(a), transient temperature profiles are shown at $X = 1$ and for different values of Sc, ε and their effect on time to reach steady state. We observe from this figure that in the absence of viscous dissipation heat, time required to reach steady state for $Sc = 0.30$, or 0.78 is either $t = 4.6$ and 6.4 respectively whereas in the presence of viscous dissipative heat, it is $t = 4.8$ and 6.8. Hence we conclude that time required to reach steady state is more when viscous dissipative heat is present. Also time to reach steady state is more as Sc increases. In Fig. 1(b), the effect of Grashof number on time to reach steady state is shown and we conclude that in the absence of viscous dissipative heat, time required to reach steady state is slightly affected by an increase in the Grashof number but in the presence of viscous dissipative heat, an increase in Grashof number leads to an increase in the time to reach steady state, which is quite significant.

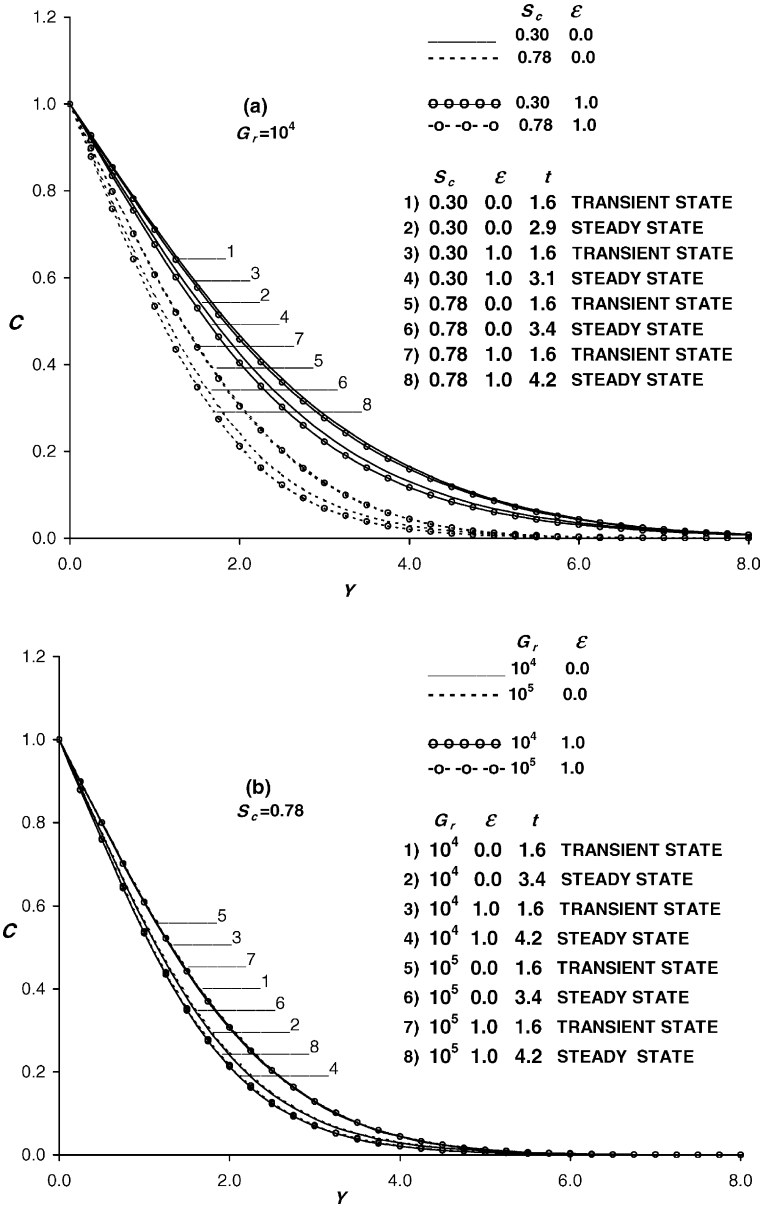

Fig. 3. Transient concentration profiles $X = 1.0$, $Pr = 0.733$, $N = 2.0$.

Again from Fig. 1(a) and (b), we observe that the transient temperature increases due to greater viscous dissipative heat, which is to be expected.

In Fig. 2, the effect of the buoyancy force and dissipation parameter on the transient temperature field is shown. In the absence of dissipation heat the steady state temperature is attained at $t = 6.4$ when N is large whereas it is attained at $t = 10.0$ when N is small. These results can be used in technological designs. Hence we conclude that in the absence of dissipative heat, time required to reach steady state decreases as the buoyancy force increases. However, at large value of N time required to reach steady state is more in the presence of viscous dissipative heat as compared to that in the absence of viscous dissipative heat. But at small value of N time required to reach steady state is less in the presence of viscous dissipative heat as compared to that in the absence of viscous dissipative heat.

Transient and steady state concentration profiles are shown for $N = 2.0$, $Gr = 10^4$ and for different values of Sc, ε In Fig. 3(a), we observe that an increase in the Schmidt number leads to a decrease in the concentration. It takes more time to reach steady state in the presence of viscous dissipative heat. Time taken to reach steady state increases with increasing Sc. In Fig. 3(b), concentration profiles are shown for different values of Gr and ε. We observe from this figure that the Grashof number does not affect the steady state time, it takes more time to reach steady state when viscous dissipative heat is present. In Fig. 4, concentration profiles are shown for different values of the buoyancy ratio force (aiding force). We observe from this figure that time required to reach steady state is more when value of buoyancy force parameter N is less. Also an increase in N leads to a fall in the concentration.

Transient and steady state velocity profiles are shown in Fig. 5(a), (b) and Fig. 6. We observe from Fig. 5(a), that an increase in the Schmidt number Sc leads to a decrease in the transient velocity. Time required to reach steady state is more when viscous dissipative heat is present or when Schmidt number is large. From Fig. 5(b), we observe that an increase in Grashof number leads to a fall in the transient velocity, but the steady state is reached late in time when the Grashof number is high and there is no viscous dissipative heat. However, in the presence of viscous dissipative heat, time required to reach steady state is more when Grashof number is large. The effect of buoyancy force is seen in Fig. 6. We observe from this figure that an increase in the buoyancy force N leads to an increase in the transient velocity. Also, time required to reach steady state is more when viscous dissipative heat is present. However, at small value of N time required to reach steady state is more in the presence of viscous dissipative heat as compared to that in the absence of viscous dissipative heat.

We now study the effects of viscous dissipative heat and the mass transfer on the local and average skin-friction, which is given by

$$\tau_L = \frac{1}{Gr^{1/4}} \left(\frac{\partial U}{\partial Y} \right)_{y=0} \tag{21}$$

$$\bar{\tau} = \frac{1}{Gr^{1/4}} \int_0^1 \left(\frac{\partial U}{\partial Y} \right)_{y=0} dX \tag{22}$$

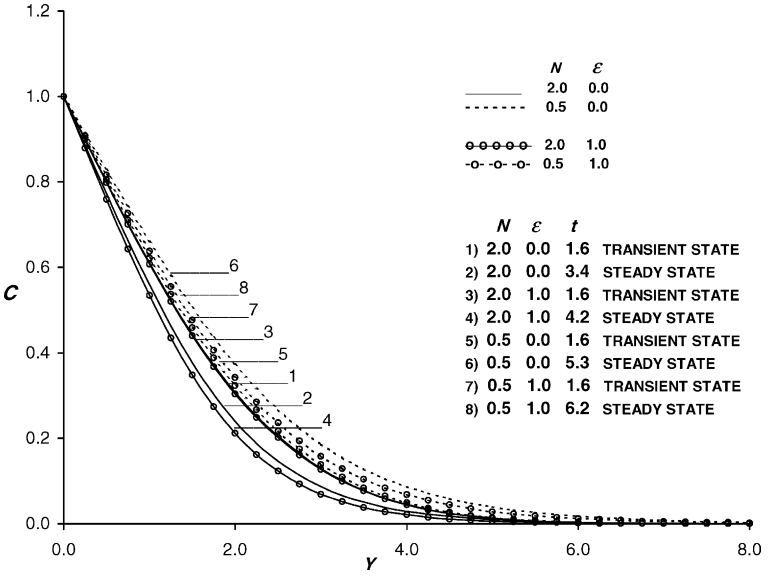

Fig. 4. Transient concentration profiles $X = 1.0$, $Pr = 0.733$, $Gr = 10^4$, $Sc = 0.78$.

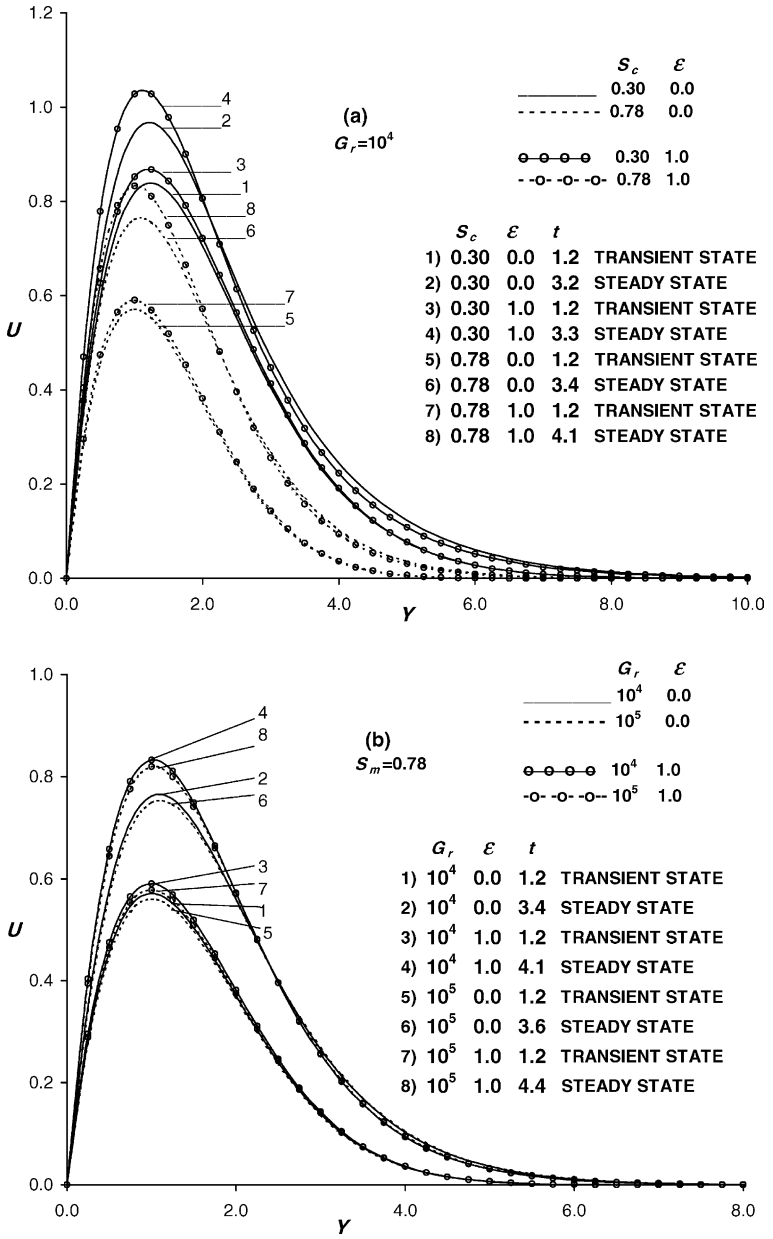

Fig. 5. Tansient velocity profiles $X = 1.0$, $Pr = 0.733$, $N = 2.0$.

The numerical values of τ_L, local skin-friction is evaluated by using five-point approximate formula for the derivative in (21) and this is shown in Fig. 7. It is observed from this figure that an increase in the buoyancy force N leads to an increase in τ_L. Greater viscous dissipative heat also causes a rise in the local skin-friction. An increase in Gr leads to a fall in the local skin-friction. Local skin-friction decreases as the Schmidt number Sc increases.

To evaluate the average skin-friction from (22), the integrand is approximated by a five-point formula and then the integral is evaluated by using Newton–Cotes closed integration formula and these are shown in Fig. 8. We observe from this figure that due to greater viscous dissipative heat, there is an increase in the average skin-friction, but average skin-friction decreases with increasing the Schmidt number or Grashof number. Again due to greater buoyancy ratio parameter, the average skin-friction increases.

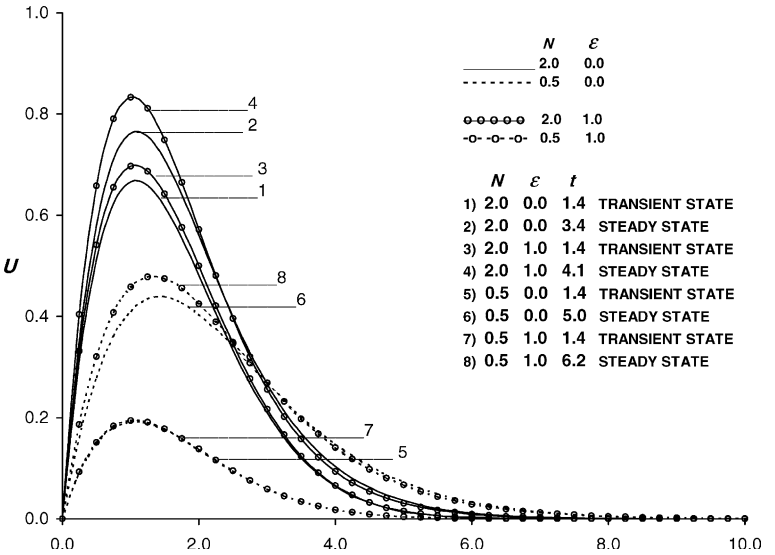

Fig. 6. Transient velocity profiles $X = 1.0$, $Pr = 0.733$, $Gr = 10^4$, $Sc = 0.78$.

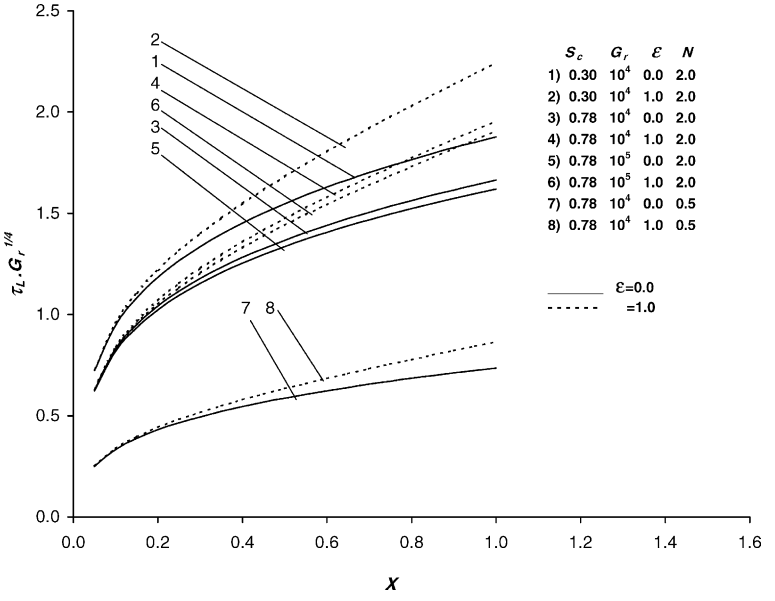

Fig. 7. Steady state local skin friction, $Pr = 0.733$.

We now study the local and average Nusselt number Nu, which is defined as

$$Nu_{XL} = Gr^{1/4}\frac{X}{\theta_w} \tag{23}$$

$$\overline{Nu_X} = Gr^{1/4}\int_0^1 \frac{dX}{\theta_w} \tag{24}$$

We have computed numerical values of steady state local Nusselt number and these are plotted in Fig. 9. We observe from this figure that local Nusselt number decreases due to the presence of viscous dissipative heat. In the absence of viscous dissipative heat, an increase in buoyancy ratio parameter N leads to an increase in the local Nusselt number, but in the presence of viscous dissipative heat, local Nusselt number decreases due to the buoyancy ratio parameter N.

An increase in Gr also leads to a decrease in the local Nusselt number. In the absence of viscous dissipative heat, an increase in the Schmidt number leads to

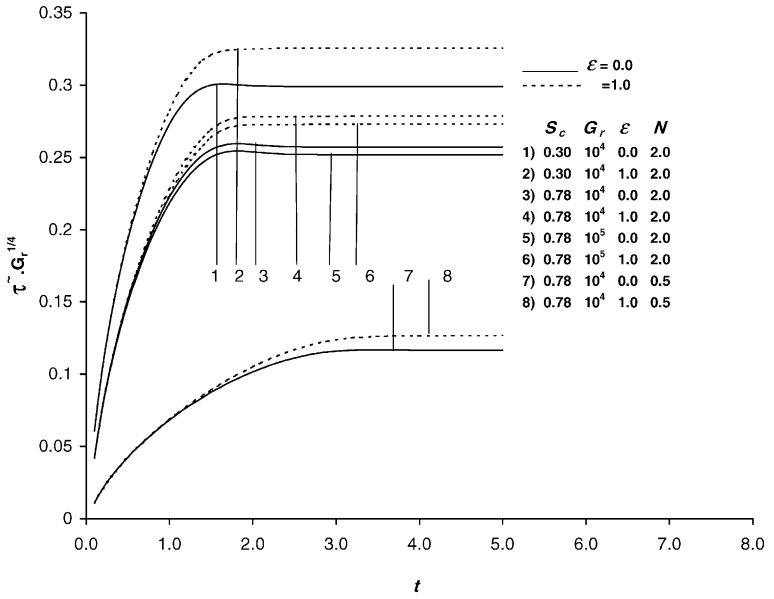

Fig. 8. Average skin friction, $Pr = 0.733$.

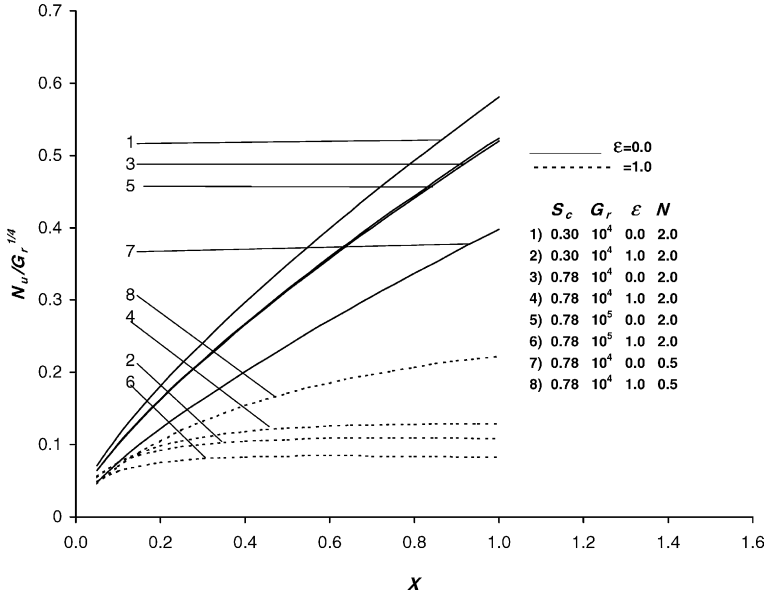

Fig. 9. Steady state local Nusselt number, $Pr = 0.733$.

a decrease in the local Nusselt number whereas in the presence of viscous dissipative heat, the local Nusselt number increases with increasing the Schmidt number.

In Fig. 10, the Average Nusselt number is shown. It is seen from this figure that the average Nusselt number decreases due to greater viscous dissipative heat. It increases with increasing the buoyancy ratio parameter N in the absence of viscous dissipative heat but decreases with increasing N in the presence of viscous dissipative heat. Due to increasing the Grashof number Gr, average Nusselt number decreases. In the absence of viscous dissipative heat, average Nusselt number decreases due to increasing the Schmidt number but in the presence of viscous dissipative heat average Nusselt number increases with increasing the Schmidt number.

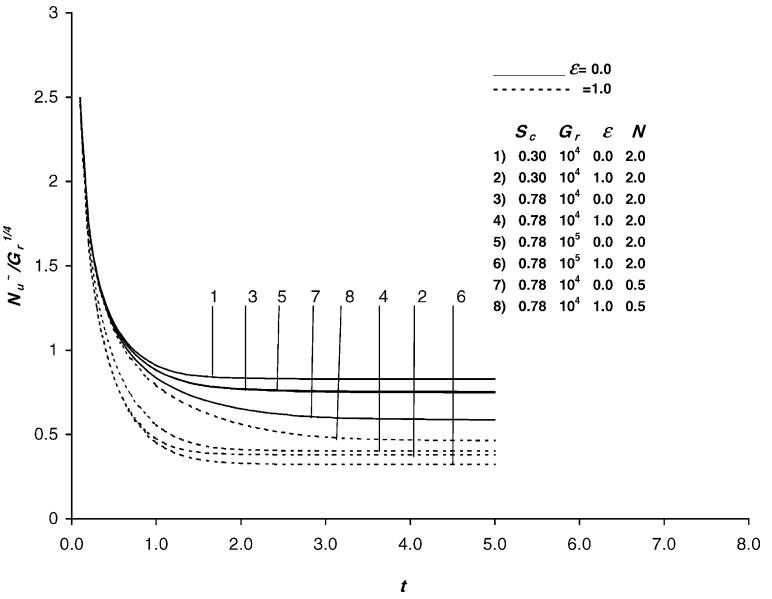

Fig. 10. Average Nusselt number, $Pr = 0.733$.

We now study the local and average Sherwood number, which is defined as

$$Sh_{XL} = -\left(\frac{\partial C}{\partial Y}\right)_{y=0} Gr^{1/4}$$
$$\overline{Sh_X} = -Gr^{1/4} \int_0^1 \left(\frac{\partial C}{\partial Y}\right)_{y-0} \mathrm{d}X \tag{25}$$

In Fig. 11, the local Sherwood number is shown and we observe from this figure that an increase in the buoyancy ratio parameter N or dissipation number ε leads to an increase in the local Sherwood number. But the local Sherwood number decreases due to increasing the Grashof number. Again the local Sherwood number increases due to increasing the Schmidt number.

The average Sherwood number is shown in Fig. 12. It is seen from this figure that the average Sherwood number increases due to greater viscous dissipative heat. It increases with increasing the buoyancy ratio

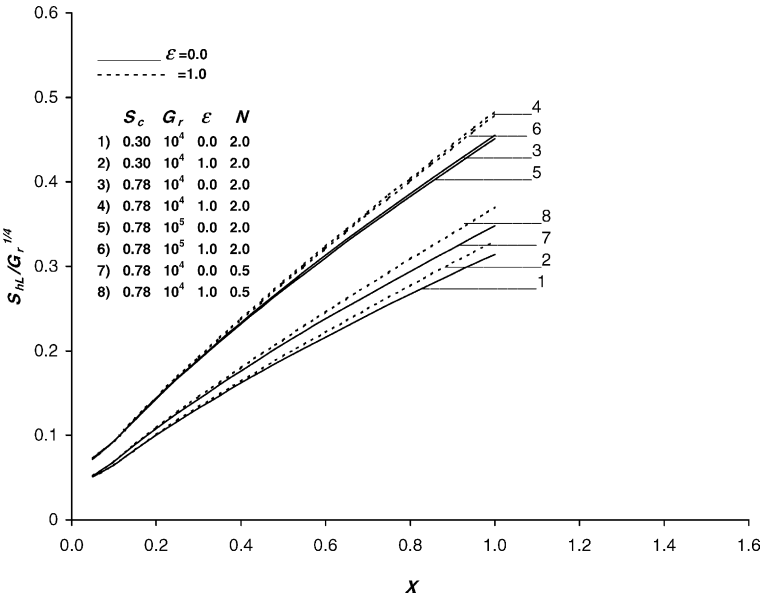

Fig. 11. Steady state local Sherwood number, $Pr = 0.733$.

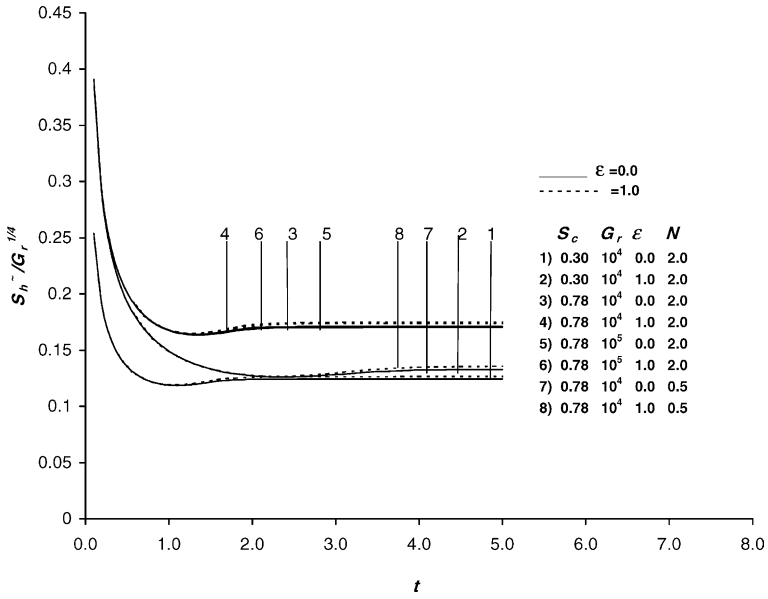

Fig. 12. Average Sherwood number, $Pr = 0.733$.

parameter N. However, Grashof number does not affect Sherwood number. Sherwood number increases with increase in the Schmidt number.

3. Conclusions

(1) Time required to reach steady state temperature is more with viscous dissipation and also with increase in *Sc* the Schmidt number.
(2) In the absence of viscous dissipation time required to reach steady state temperature is slightly affected by increasing the value of Grashof number. But in the presence of viscous dissipative heat, an increase in Grashof number leads to an increase in the time to reach steady state, which is very significant.
(3) As the buoyancy force increases, there is a decrease in the time to reach steady state.
(4) In the presence of viscous dissipative heat, more time is required to reach the steady state temperature, than that in the absence of viscous dissipative heat for large value of N.
(5) An increase in the Schmidt number leads to a decrease in concentration.
(6) Time required to reach steady state concentration increases with increase in Schmidt number and it also increases with viscous dissipation.
(7) Grashof number does not affect the time to reach steady state concentration.
(8) Time required to reach steady state concentration is more when the value of buoyancy force parameter N is less.
(9) An increase in *Sc* leads to a decrease in transient velocity.
(10) Time required to reach steady state velocity is more when viscous dissipative heat is present or Schmidt number is large.
(11) An increase in Grashof number leads to a fall in the transient velocity.
(12) The steady state velocity is reached late in time when the Grashof number is high.
(13) Greater viscous dissipative heat causes a rise in local as well as average skin-friction, but there is a fall in these values as Schmidt number *Sc* increases.
(14) Local and average Nusselt numbers decrease with greater viscous dissipative heat.
(15) Local and average Sherwood numbers increase slightly due to presence of viscous dissipative heat, but there is substantial rise in their values with an increase in the value of Schmidt number.

References

[1] B. Gebhart, Y. Jaluria, R.L. Mahajan, B. Sammakia, Buoyancy-induced Flows and Transport, Springer-Verlag, Berlin, 1988.
[2] E. Pohlhausen, Der Warmeaustausch Zwischen Festen Korpern und Flussigkeiten mit Kleiner Reibung und Kleiner Warmeleitung, ZAMM 1 (1921) 115–125.
[3] S. Ostrach, An analysis of laminar free convection flow and heat transfer about a flat plate parallel to the direction of the generating body force, NACA Report, 1111 (1953).

[4] B. Gebhart, Effects of viscous dissipation in natural convection, J. fluid Mech. 14 (1962) 225–232.
[5] G.D. Callahan, W.J. Marner, Transient free convection with mass transfer on an isothermal vertical flat plate, Int. J. Heat Mass Transfer 19 (1976) 165–174.
[6] V.M. Soundalgekar, P. Ganesan, Transient free convection flow on a semi-infinite vertical plate with mass transfer, Reg. J. Energy Heat Mass Transfer 2 (1980) 83–91.
[7] V.M. Soundalgekar, P. Ganesan, Finite difference analysis of transient free Convection on an isothermal vertical flat plate, Reg. J. Energy Heat Mass Transfer 3 (1981) 219–224.
[8] V.M. Soundalgekar, P. Ganesan, Finite difference analysis of transient free convection with mass transfer on an isothermal vertical flat plate, Int. J. Engng. Sci. 19 (1981) 757–770.
[9] V.M. Soundalgekar, P. Ganesan, Finite difference analysis of transient free Convection flow past a vertical flat plate with constant heat flux, in: Proceedings of 2nd International Conference On Numerical Methods in Thermal problem, July 7-10, Venice, 1981, pp. 1096–1107.
[10] V.M. Soundalgekar, B.S. Jaiswal, A.G. Uplekar, H.S. Takhar, Transient free convection flow of a viscous dissipative fluid past a semi-infinite vertical plate, J. Appl. Mech. Engng. 4 (1999) 203–218.
[11] B. Carnahan, H.A. Luther, J.O. Wilkes, Applied Numerical Methods, John Wiley, New York, 1969.
[12] B. Gebhart, L. Pera, The nature of vertical natural convection flows resulting from the combined buoyancy effects of thermal and mass diffusion, Int. J. Heat Mass Transfer 14 (1971) 2025–2050.